

Neuronal heterogeneity modulates phase synchronization between unidirectionally coupled populations with excitation-inhibition balance

Katiele V. P. Brito and Fernanda S. Matias^{*}*Instituto de Física, Universidade Federal de Alagoas, Maceió, Alagoas 57072-970, Brazil*

(Received 26 November 2020; accepted 2 March 2021; published 31 March 2021)

Several experiments and models have highlighted the importance of neuronal heterogeneity in brain dynamics and function. However, how such a cell-to-cell diversity can affect cortical computation, synchronization, and neuronal communication is still under debate. Previous studies have focused on the effect of neuronal heterogeneity in one neuronal population. Here we are specifically interested in the effect of neuronal variability on the phase relations between two populations, which can be related to different cortical communication hypotheses. It has been recently shown that two spiking neuron populations unidirectionally connected in a sender-receiver configuration can exhibit anticipated synchronization (AS), which is characterized by a negative phase lag. This phenomenon has been reported in electrophysiological data of nonhuman primates and human EEG during a visual discrimination cognitive task. In experiments, the unidirectional coupling could be accessed by Granger causality and can be accompanied by either positive or negative phase difference between cortical areas. Here we propose a model of two coupled populations in which the neuronal heterogeneity can determine the dynamical relation between the sender and the receiver and can reproduce phase relations reported in experiments. Depending on the distribution of parameters characterizing the neuronal firing patterns, the system can exhibit both AS and the usual delayed synchronization regime (DS, with positive phase) as well as a zero-lag synchronization regime and phase bistability between AS and DS. Furthermore, we show that our network can present diversity in their phase relations maintaining the excitation-inhibition balance.

DOI: [10.1103/PhysRevE.103.032415](https://doi.org/10.1103/PhysRevE.103.032415)

I. INTRODUCTION

The coherent activity of different cortical areas has been considered related to numerous cognitive functions, such as object recognition, visual-motor integration, and working memory [1,2]. Many hypotheses about neuronal communication take into account the role of brain oscillation and phase synchronization, for example, the binding by synchrony [3], the communication through coherence [4,5], the gating by inhibition [6], and nested oscillations [7]. Although the mechanisms involved in large-scale integration are still unknown, they have been extensively studied with biologically inspired neuronal population models [8].

Spiking neurons are typically considered the building blocks of the population dynamics, and neuronal diversity is ubiquitous across the nervous system. However, the functional significance of neuronal heterogeneity is still under investigation [9–13]. From the experimental point of view, empirical observations show considerable variability in the response properties of different neurons [12,14,15] and its relation with efficient neural coding [9]. From the modeling side, a variety of computational network models of one neuronal population have been employed to study the effect of heterogeneity in synchronization and coding capabilities [16–21], in self-sustained activity [22], and in persistent activity, which could underlie the cognitive function of working memory [23,24].

The previous studies mentioned above have investigated the effect of neuronal heterogeneity in one neuronal popu-

lation. Here we are interested in the role of heterogeneity in the phase synchronization of a physiologically plausible model of two neuronal populations unidirectionally coupled. This could be potentially useful to understand the influence of neuronal variability on the communication between distant brain areas [3–7]. The neuronal population model studied here has been employed before, in the light of anticipated synchronization ideas [25,26], to explain electrophysiological results in nonhuman primates showing that unidirectional Granger causality can be accompanied by either positive or negative phase difference between cortical areas [26–29]. However, the effect of neuronal variability on those phase relations has not been explored.

The typical synchronized regime between two unidirectionally coupled systems exhibits a positive phase lag in which the sender is also the leader. This regime is usually called delayed synchronization (DS) or simply lagged synchronization. However, it has been shown that the sender-receiver configuration can also synchronize with a negative phase lag if the system can be described by the following equations in which the receiver is subjected to a delayed self-feedback [25]:

$$\begin{aligned}\dot{\mathbf{S}} &= \mathbf{f}(\mathbf{S}(t)), \\ \dot{\mathbf{R}} &= \mathbf{f}(\mathbf{R}(t)) + \mathbf{K}[\mathbf{S}(t) - \mathbf{R}(t - t_d)].\end{aligned}\quad (1)$$

The stable solution $\mathbf{R}(t) = \mathbf{S}(t - t_d)$ characterizes the counterintuitive situation in which the receiver leads the sender, and it is called anticipated synchronization (AS). This means that the activity of the receiver predicts the activity of the sender by an amount of time t_d . In the last 20 years, this solution has been extensively studied in physical systems both

*fernanda@fis.ufal.br

theoretically [25,30–35] and experimentally [36–38]. In particular, AS in unidirectional circuits has been employed for control and prediction of undesirable events [37].

It has been shown that AS can also occur if the delayed self-feedback is replaced by different parameter mismatches at the receiver [39–41], a faster internal dynamics of the receiver [42–45], as well as an inhibitory loop mediated by chemical synapses [46–49]. Moreover, when the feedback is not hard-wired in the equation but emerges from system dynamics, two neuronal population can present phase diversity and a transition from AS to DS through zero-lag synchronization, induced by synaptic properties [26,45]. Different patterns of phase synchronization can also emerge due to the time delays in heterogeneous networks [50]. More recently, it has been shown that a sender-receiver network can also present phase bistability between DS and AS regimes [51]. It is worth mentioning that in symmetric bidirectional coupled systems it is not possible to separately classify AS or DS, but only a lagged synchronization. In case of asymmetric bidirectional influence we can define the stronger direction of influence as the sender-receiver direction. For example, the effect of a bidirectional connection in the AS regime has been studied in neuronal motifs coupled by chemical synapses [47]. Since chemical synapses are unidirectional by their own nature, in such circuits each direction of influence is independent of one another.

Here we show that the neuronal heterogeneity can promote diversity of phase relations between two neuronal networks with an excitation-inhibition balance. As far as we know, this is the first verification that the neuronal spiking properties of the population can promote AS and phase bistability. In Sec. II we describe the neuronal population model as well as the parameters that we use to change neuronal heterogeneity. In Sec. III we report our results, showing that the motif can exhibit phase-locking regimes: with positive, negative, and zero phases and a bistable regime which alternates from AS to DS. We also show that the excitatory and inhibitory conductances remain with a fixed relationship during oscillations. Concluding remarks and a brief discussion of the significance of our findings for neuroscience are presented in Sec. IV.

II. NETWORK MODEL WITH NEURONAL HETEROGENEITY

A. Each node is a neuron model with a specific firing pattern

Our neuronal motif is composed of two unidirectionally coupled cortical-like neuronal populations: a sender (S) and a receiver (R); see Fig. 1. Each one is composed of 400 excitatory and 100 inhibitory neurons [26], which is the typical employed proportion of 80% excitatory neurons and 20% inhibitory neurons, based on anatomical estimates for the neocortex [52]. Each neuron is described by the Izhikevich model [53]:

$$\frac{dv}{dt} = 0.04v^2 + 5v + 140 - u + \sum_x I_x, \quad (2)$$

$$\frac{du}{dt} = a(bv - u). \quad (3)$$

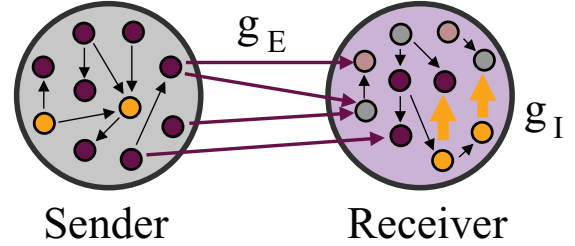


FIG. 1. Schematic representation of two cortical areas, composed of hundreds of spiking neurons and chemical synapses, coupled in a sender-receiver configuration. Both populations have neuronal heterogeneity, but for the receiver (R) population we vary the distribution of parameters determining the neuronal firing patterns. The inhibitory feedback is controlled by the synaptic conductance g_I at R, whereas the sender-receiver coupling is determined by excitatory synaptic conductances with g_E .

In Eqs. (2) and (3) v is the membrane potential and u the recovery variable which accounts for activation of K^+ and inactivation of Na^+ ionic currents. I_x are the synaptic currents provided by the interaction with other neurons and external inputs. If $v \geq 30$ mV, v is reset to c and u to $u + d$.

To study the effects of neuronal variability at the receiver population, we use different values of c and d for the excitatory neurons in R:

$$c = -55 - X + [(5 + X)\sigma^2] - [(10 - X)\sigma^2], \quad (4)$$

$$d = 4 + Y - [(2 + Y)\sigma^2] + [(4 - Y)\sigma^2]. \quad (5)$$

We use $Y = 2X/5$ to guarantee that the neuronal-type distribution is changing from regular spikes (RS, $c = -65$ and $d = 8$) to chattering (CH, $c = -50$ and $d = 2$) via intrinsically bursting (IB, $c = -55$ and $d = 4$) neurons. As we vary X from -5 to 10 the number of neurons of each type in the R population changes as shown in Fig. 2. We vary X throughout the paper to show how heterogeneity can affect phase relations between the two populations. Illustrative examples of neuronal firings embedding in the neuronal population but with different parameters are shown in Fig. 3. Equations were integrated with the Euler method and a time step of 0.05 ms.

B. Each link is an excitatory or inhibitory chemical synapse

The connections between neurons in each population are assumed to be fast unidirectional excitatory and inhibitory chemical synapses mediated by AMPA and GABA_A. The synaptic currents are given by

$$I_x = g_x r_x (v - V_x), \quad (6)$$

where $x = E, I$ (excitatory and inhibitory mediated by AMPA and GABA_A, respectively), $V_E = 0$ mV, $V_I = -65$ mV, g_x is the synaptic conductance maximal strengths, and r_x is the fraction of bound synaptic receptors whose dynamics is given by

$$\tau_x \frac{dr_x}{dt} = -r_x + D \sum_k \delta(t - t_k), \quad (7)$$

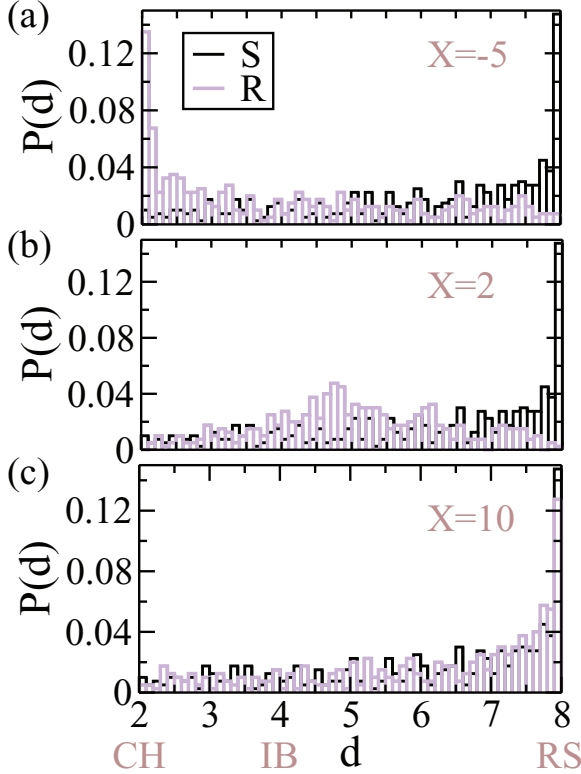


FIG. 2. Probability distribution of finding an excitatory neuron at the R population with model parameter d , which determines its spiking firing pattern [see Eqs. (4) and (5)]. (a) For $X = -5$ it is very probable to find $d = 2$ (and consequently $c = -50$), which ensures that there are more chattering (CH) neurons in the population than other neuron types. (b) For $X = 2$ the distribution of d has a peak around $d = 5$, and there are more intrinsically bursting (IB) neurons ($d = 4$ and $c = -55$) than other kinds. (c) For $X = 10$ the majority of neurons are regular spiking (RS, $d = 8$ and $c = -65$).

where the summation over k stands for presynaptic spikes at times t_k . D is taken, without loss of generality, equal to 0.05. The time decays are $\tau_E = 5.26$ ms $\tau_I = 5.6$ ms. Each neuron is subject to an independent noisy spike train described by a Poisson distribution with rate R . The input mimics excitatory synapses (with conductances g_P) from n presynaptic neurons external to the population, each one spiking with a Poisson rate R/n , which, together with a constant external current I_c , determines the main frequency of mean membrane potential of each population. Unless otherwise stated, we have employed $R = 2400$ Hz and $I_c = 0$.

Connectivity within each population randomly targets 10% of the neurons, with excitatory conductances set at $g_E^S = g_E^R = 0.5$ nS. Inhibitory conductances are fixed at the sender population $g_I^S = 4.0$ nS, and g_I at the receiver population is varied throughout the study (see Fig. 1). Each neuron at the R population receives 20 fast synapses (with conductance g_E) from random excitatory neurons of the S population. It is worth emphasizing that to analyze the excitation-inhibition balance at each neuron, we use $G_x = g_x r_x$ as the effective synaptic conductance at each time step, which is a fraction of the maximal possible value of g_x .

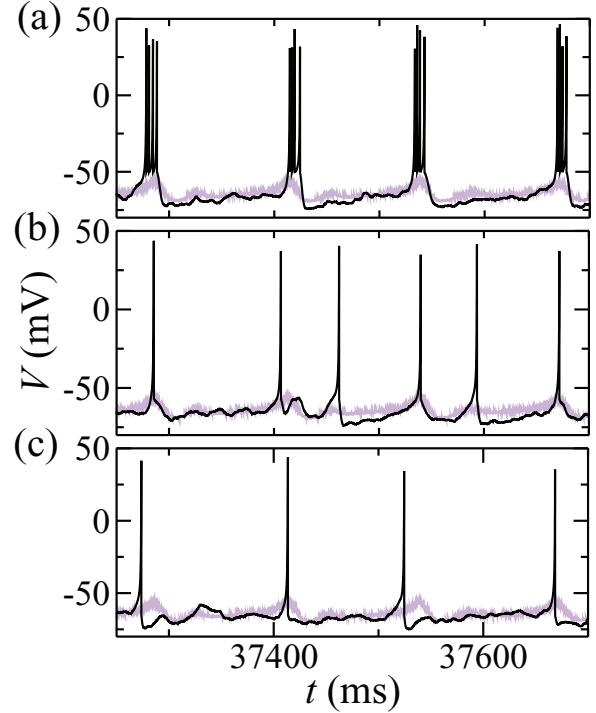


FIG. 3. Three exemplar neuronal time series to illustrate neuronal heterogeneity embedded in the network. Firing pattern during the oscillatory activity of (a) a chattering neuron (CH, $c = -50.4$), (b) an intrinsically bursting neuron (IB, $c = -56.9$), and (c) a regular spiking neuron (RS, $c = -64.9$). The purple line shows the mean activity of all neurons in the same population (for fixed $X = 2$ and $g_I = 2.0$ nS).

C. Characterizing phase relations between sender and receiver populations

Since the mean membrane potential V_x ($x = S, R$) of each population (which we assume as a crude approximation of the measured LFP) is noisy, we average within a sliding window of width 5–8 ms to obtain a smoothed signal, from which we can extract the peak times $\{t_i^x\}$ (where i indexes the peak). The period of a given population in each cycle is thus $T_i^x \equiv t_{i+1}^x - t_i^x$. For a sufficiently long time series, we compute the mean period T_x and its variance.

In a similar way we calculate the time delay in each cycle $\tau_i = t_{i+1}^R - t_i^S$. Then, if τ_i obeys a unimodal distribution, we calculate τ as the mean value of τ_i and σ_τ as its variance. If $T_S \approx T_R$ and g_E is independent of the initial conditions, the populations exhibit oscillatory synchronization with a phase-locking regime. We indistinguishably use the term phase difference or time delay since it is always possible to associate both: $\phi_i = 2\pi \tau_i / T_S$. In all these calculations we discard the transient time.

It is also possible to estimate the time delay by using the peak of the delayed cross-correlation function $C(V_S, V_R, \Delta t)$ between the the mean membrane potential of the S and R populations. This function can be calculated as

$$C(V_S, V_R, \Delta t) = \frac{(\sum V_S^i - \bar{V}_S)(\sum V_R^{i+\Delta t} - \bar{V}_R)}{\sqrt{\sum (V_S^i - \bar{V}_S)^2} \sqrt{\sum (V_R^i - \bar{V}_R)^2}}. \quad (8)$$

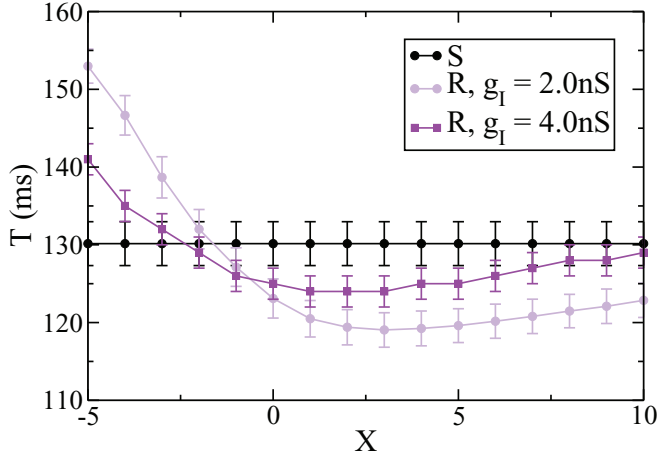


FIG. 4. Effect of neuronal heterogeneity in the oscillatory period of one population. The S and R populations are uncoupled ($g_E = 0$ nS), and by changing X , we change only the neuronal parameters c and d of neurons in the R population [see Eqs. (4) and (5)]. The oscillatory period of R depends on both inhibition and the neuronal variability parameter X .

The values of $C(V_S, V_R, \Delta t)$ also indicate the level of synchronization between the two populations.

III. RESULTS

A. The effect of neuronal heterogeneity in one population

To study the effect of neuronal heterogeneity in the oscillatory properties of only one population, we analyze the uncoupled case ($g_E = 0$). For comparison, the Sender population, which has a fixed distribution of neuronal spiking types, oscillates with a mean period of $T_S = 130$ ms. As we change the neuronal types distribution of the Receiver population by varying X in Eq. (4), the oscillatory period of R varies from more than 150 ms to less than 120 ms (see Fig. 4 for two different values of inhibition: $g_I = 2.0$ nS and $g_I = 4.0$ nS). A decrease in the number of chattering neurons and an increase in the number of intrinsically bursting neurons facilitate faster oscillations.

This means that we can control the internal dynamics of the population by changing the local properties of the neurons. In particular, we can turn the receiver faster maintaining the excitation-inhibition balance by changing X . It is worth mentioning that the E/I balance has been extensively related to network dynamics, information processing in the nervous system, and social dysfunction [54–56]. Moreover, it was not always possible to keep the E/I balance in previous studies in which the internal dynamics of the receiver were determined by the relationship between inhibitory and excitatory synaptic currents at the receiver [45,51].

B. Local properties at the receiver population modulates global phase relations between two populations

The free-running properties of each population can influence the synchronization patterns between them when we turn the sender-receiver coupling on ($g_E > 0$) [43–45]. In fact, for $g_E = 0.5$ nS and $g_I = 2.0$ nS the motif can exhibit

three different regimes depending on X . Illustrative examples of these dynamics are shown in Fig. 5 for $X = -5$, $X = 2$, and $X = 10$. The distribution of neuronal spiking parameters shown in Fig. 2 ensures that the receiver population exhibits more chattering neurons for $X = -5$, more intrinsically bursting neurons for $X = 2$, and more regular spiking neuron for $X = 10$. For $X = -5$ the system presents the usual phase-locking regime with positive mean time delay $\tau = 13$ ms. This means that a peak of the mean membrane potential of the sender population is followed by a peak of the receiver. Therefore, the time delay in each cycle τ_i is positive and fluctuates around a well-defined mean value (see the left column in Fig. 5). For this example, the delayed cross-correlation function $C(V_S, V_R, \Delta t)$ calculated by Eq. (8) has a local peak of 0.92 for $\Delta t = 15$ ms.

For $X = 10$, a peak of the Sender is, for the majority of the cycles, preceded by a peak of the receiver ($\tau_i < 0$), and, consequently, the mean time delay is negative (see the right column in Fig. 5). This characterizes the anticipated synchronization regime (AS, with mean time delay $\tau = -39$ ms for this example). This counterintuitive regime explains the observed unidirectional influence with negative phase difference verified in local field potential (LFP) monkey data [26,28,29] as well as in human EEG [57]. Moreover, AS could be possibly related to commonly reported short latency in visual systems [58–63], olfactory circuits [64], songbird brain [43], and human perception [65,66]. For this example, the delayed cross-correlation function $C(V_S, V_R, \Delta t)$ has a local peak of 0.84 for $\Delta t = -39$ ms.

For intermediate values of X the system exhibits a phase bistability between these two possible phase-locking regimes: DS and AS [see Figs. 5(b), 5(e), and 5(h) with $X = 2$]. The activity alternates from a few periods of DS eventually followed by a few periods of AS. In other words, the time delay τ_i is positive for a few cycles, with a well-defined mean value and standard deviation (close to $\tau = 4.5$ ms in this case), which is similar to a DS regime for a certain amount of periods. Then the system randomly switches to a different dynamics in which τ_i is negative during a few other cycles (the mean time delay is close to $\tau = -36$ ms for this example). Therefore, in this regime, the system cannot be simply characterized by the mean time delay (τ).

A phase bistability between AS and DS has been previously reported for very small values of inhibition [51]. It has been proposed that this phase bistability could be a plausible model for differences in phase synchronization of MEG data during bistable perception [67]. Kosem *et al.* [67] have shown that when participants are listening to bistable (or ambiguous) speech sequences that could be perceived as two distinct word sequences repeated over time, their MEG recordings present phase differences related to which sequence they are perceiving. Therefore, we propose that this phase bistability can also be promoted by neuronal variability in cortical regions.

The three different regimes can also be visualized in a raster plot as in Fig. 6. In these plots, each dot represents a spike of the i th neuron indexed by the vertical axis at the time indicated by the horizontal axis. It is worth mentioning a few points. Interneurons (indices 400 to 499) are spiking with higher frequency than excitatory neurons (indices 0 to 399) in both populations. The spiking pattern of the

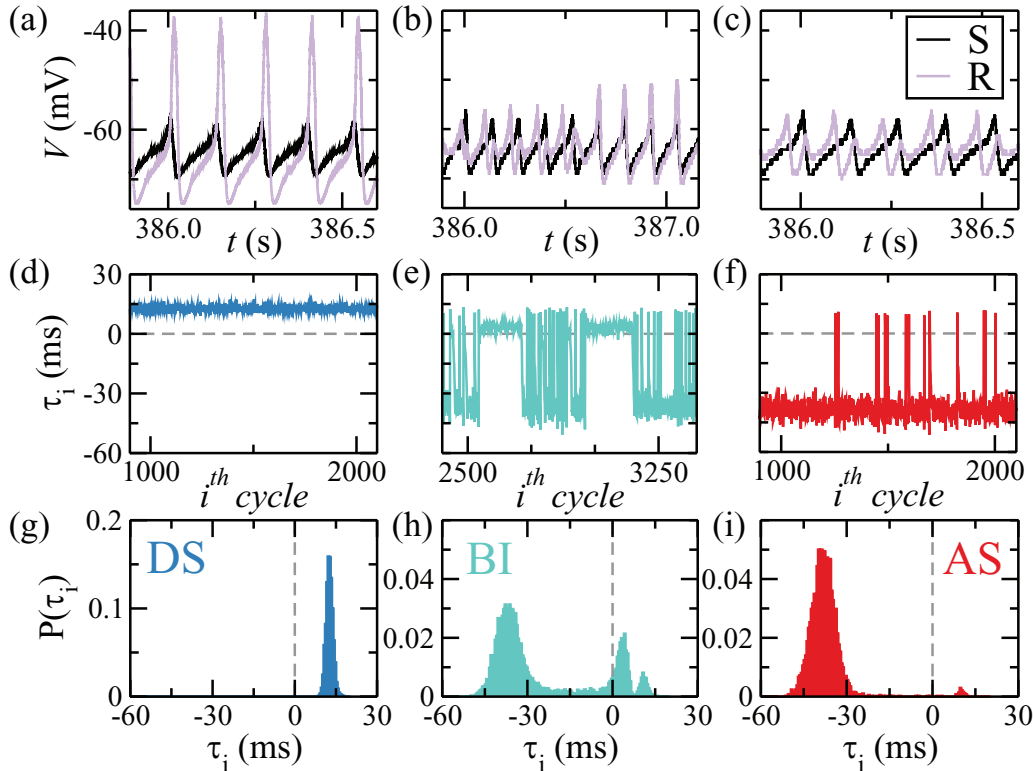


FIG. 5. Characterizing the three different dynamical regimes exhibited by the two neuronal populations depending on the parameter X controlling the neuronal spiking variability. There are two possible phase-locking regimes: delayed synchronization (DS, $X = -5$) and anticipated synchronization (AS, $X = 10$), as well as a bistable regime in respect to the phase differences (BI, $X = 2$). (a–c) Time series for sender and receiver populations. (d–f) Time delay τ_i per cycle. (g–i) Probability distribution of time delays. (g) The unimodal distribution with a positive average characterizes DS, whereas (i) the negative average represents AS. (j) The bimodal distribution together with an alternation between cycles of DS randomly followed by cycles of AS characterizes the phase bistability. Synaptic conductances are kept fixed: $g_E = 0.5$ nS and $g_I = 2.0$ nS.

excitatory neurons at the receiver population in the DS regime is more concentrated close to the peak of the mean activity. This means that the neurons are more synchronized with each other. On the other hand, the variability along the entire period is larger in the AS regime. Bursting neurons and regular spiking neurons can more easily fire in the middle of the period than chattering neurons (see an example in Fig. 3). Since we are changing the proportion of CH, IB, and RS neurons to obtain the transition from one regime to another, we could speculate that CH neurons facilitate the synchronization of the entire population and the usual DS regime, whereas RS neurons allow the observed larger diversity and the AS regime.

By incremental changes in the neuronal heterogeneity, the system can undergo a transition from DS to AS through the bistable regime or via zero lag synchronization depending on the amount of inhibition at the receiver. Figure 7 shows the mean time delay as a function of X , the parameter controlling the neuron-type distribution, for different values of inhibitory conductance g_I . Each curve corresponds to a horizontal line in Fig. 8, which displays a two-dimensional projection of the parameter space of our model (X, g_I).

For $g_I > 4.5$ nS the transition from DS to AS is continuous, and we can find virtually any value of mean time delay between the two populations, including a zero-lag synchronization, in which the peak of activity of both regions occurs very close on average (see $g_I = 5$ nS and $g_I = 6$ nS in Fig. 7).

In Fig. 8 we can see that the end of the bistable regime between DS and AS gives way to a DS-AS transition via zero lag and coincides with a change in the slope of the boundary between DS and AS. This reentrant behavior allows the system to have, for example, for fixed $X = 1$, a first DS-AS transition via bistability followed by an AS-DS transition via zero lag as a function of g_I (this would correspond to a vertical line $X = 1$ in Fig. 7).

The zero-lag regime has been extensively studied as a nonintuitive regime that can overcome the synaptic delays between distant areas [68,69]. The first experimental results for the total synchronization of distant neurons originated many theories about neuronal communication as binding by synchrony [3] and communication through coherence [4]. With new experimental results about phase relation diversity, the latter hypothesis has been adapted to include the effect of nonzero phase relations [5,70,71]. Furthermore, it has been shown that in unidirectionally coupled cortical populations the DS-AS transition via zero lag can be mediated by synaptic conductances [26,45] and that spiking-timing-dependent plasticity can promote auto-organized zero-lag synchronization [72].

It is worth emphasizing that previous experimental studies with brain signals have shown that unidirectional influence can be accompanied by positive, zero or negative phase differences in different frequency bands [26,28,29,57]. In our

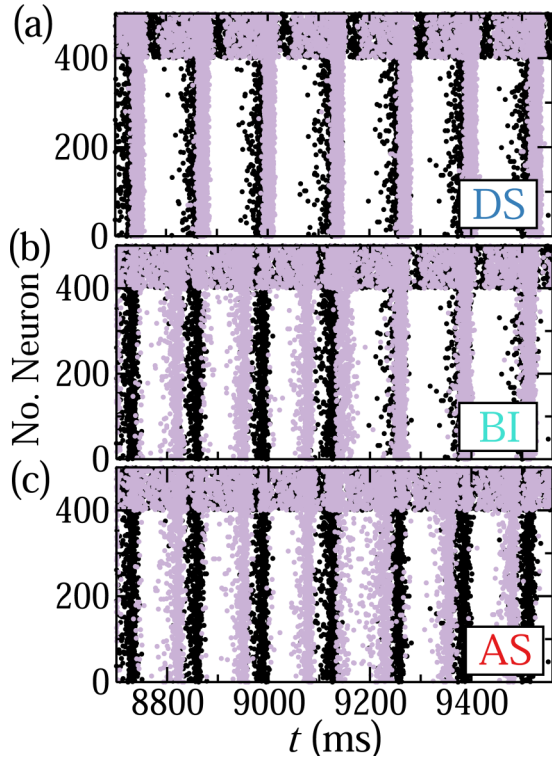


FIG. 6. Illustrative examples of the raster plots for all neurons in each dynamical regime. Black dots are neurons from the sender population, and purple (light gray) dots are neurons at the receiver. All parameters as in Fig. 5, and we change only the distribution of CH, IB, and RS spiking neurons in the network: $X = -5$ generates DS, $X = 2$ promotes the phase bistability, and for $X = 10$ the motif exhibits AS.

model, the populations oscillate with a period of 130 ms, which is equivalent to a frequency close to 7.7 Hz. This means that the time delay of 13 ms in the DS regime shown in Fig. 5(a) is equivalent to a phase delay of 0.2π rad, whereas

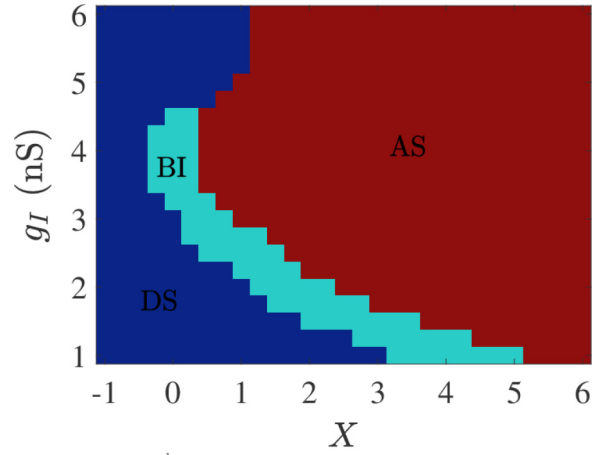


FIG. 8. Scanning parameter space to visualize the phase relation as a function of inhibitory conductance g_I and the parameter controlling neuronal variability X . The three regimes, DS, AS, and BI, can be verified for a reasonable set of parameters. Horizontal lines for integer values of g_I are shown in Fig. 7.

the anticipation in Fig. 5(c) has a phase delay of -0.6π rad. Therefore our model is able to reproduce unidirectional influence in the alpha band with both positive, zero, and negative phase relations. It has been recently shown that human EEG can present unidirectional influence between signals with both positive and negative phase relation [57]. All the 11 analyzed volunteers presented pairs of electrodes synchronized in the alpha band (from 7 to 13 Hz) with unidirectional influence and a diversity of phase relations including positive, negative, and zero phase lags. Two other studies with monkey LFP have shown that unidirectional influence can be accompanied by the counterintuitive negative phase difference reported here. Brovelli *et al.* [28] have shown that somatosensory motor cortex can influence motor cortex during oscillatory activity with main frequency around 24 Hz and a negative time difference of -8.7 ms. In a different experiment [29], it has been shown the posterior parietal cortex can unidirectional influence the prefrontal cortex in a frequency of 17 Hz and present a time difference that can range from 2.45 ms to 6.53 ms.

C. Excitation-inhibition balance

In previous studies [26,45] with sender-receiver populations, the different regimes were achieved by changing the excitation-inhibition relation via modifications in the internal inhibition, the sender-receiver coupling, or the amount of external noise simulated as excitatory synapses. In particular, the bistable regime reported in Ref. [51] required very small values of inhibitory conductance. Here we can obtain different phase relations ensuring that the excitation-inhibition balance is maintained by changing only the neuronal heterogeneity.

We can see the excitatory-inhibitory balance in Fig. 9, where the two effective synaptic conductances are plotted against each other for four different neurons of the receiver population: one chattering, one intrinsically bursting, one regular spiking, and an inhibitory neuron. These plots yield a linear relationship, which means that the excitatory and

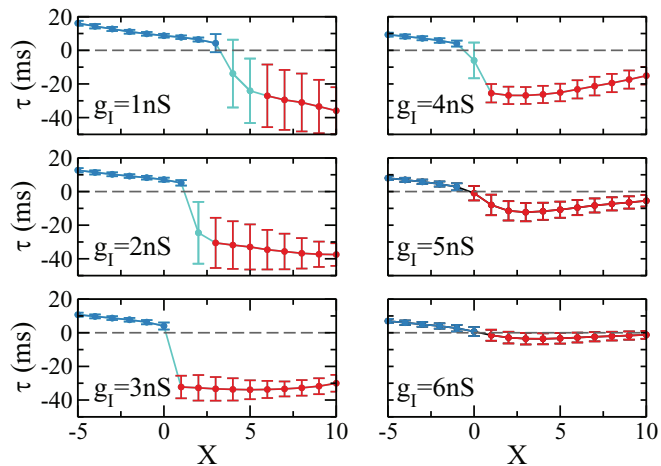


FIG. 7. Mean time delay τ between neuronal population as a function of the parameter controlling the neuronal heterogeneity X . The DS-AS transition can occur via a bistable regime or through zero-lag synchronization for sufficient large inhibition ($g_I = 5$ nS and $g_I = 6$ nS).

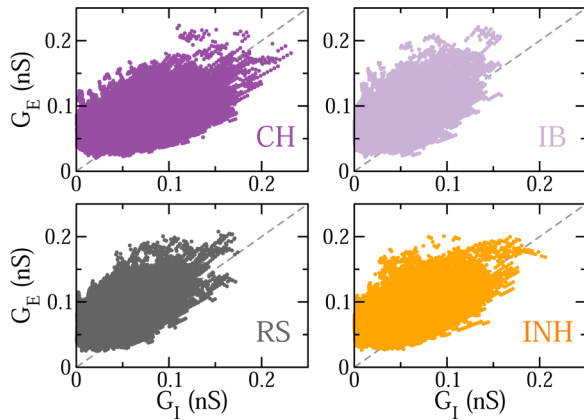


FIG. 9. Excitatory-inhibitory balance for four illustrative neurons (three excitatory, CH, IB, RS, and one inhibitory) at the receiver population during the bistable regime ($X = 2$ and $g_I = 2$ nS). Excitatory and inhibitory effective synaptic conductances preserve an approximate proportional relation to each other in the course of the oscillations.

inhibitory synaptic conductance increase and decrease in time in such a way that the ratio of the two G_E/G_I remains almost fixed. This ratio slightly varies from neuron to neuron. The E/I balance has been related to a variety of dynamical features such as oscillatory activity [54,73], information processing and social dysfunction [56], as well as cortical complexity [74].

IV. CONCLUDING REMARKS

We have shown that neuronal heterogeneity can promote different phase relations between spiking neuron networks. We have verified that by changing the proportion of different types of neuronal firing patterns the system can present phase-locking regimes with positive (DS), negative (AS), and zero phase differences as well as a bistable regime. The DS-AS transition could possibly explain commonly reported short latency in visual systems [58–63], olfactory circuits [64], songbird brain [43], and human perception [65,66], whereas

the bistable regime can be associated with bistable perception during ambiguous stimulation [51,67]. Previous studies on AS [26,45] and phase bistability [51] in the neuronal population have not explored the effects of neuronal properties on the network dynamics. Moreover, the possibility of changing the neuronal variability allows us to remain in the excitation-inhibition balance, which has been considered a fundamental property of the health brain [54,56,73,74].

Although examples of neuronal variability exist throughout the brain, their importance for the information process remains a source of debate. The functional roles of intrinsic neuronal heterogeneity on the network dynamics have been more extensively studied in the last few years [9–13]. Theoretically, the effect of heterogeneity on synchronization properties of only one neuronal network has been studied in different models [16,18–21]. In particular, Rossi *et al.* [21] argued that their results can be important in the light of communication through coherence ideas [4,5]. Here we take a step further in this direction by showing the specific effect of heterogeneity in the phase synchronization patterns of two coupled networks. In such a case, we could investigate the effect of neuronal heterogeneity in phase relations and, consequently, in communication between distant cortical areas.

Differently from the first papers about AS [25,32], here the anticipation time is not hard-wired in the dynamical equations, neither associated with the excitation-inhibition relation, but rather emerges from the neuronal dynamics and heterogeneity. This opens new possibilities to study how neuronal variability modulates the phase relation diversity between cortical areas, which has been the object of more intense investigation in the last few years [70,71]. In particular, including effects from homeostasis and the variability of inhibitory neurons are natural next steps that we are currently pursuing.

ACKNOWLEDGMENTS

The authors thank Caroline Garcia Forlim for helpful discussions and careful reading of the manuscript. The authors thank FAPEAL, UFAL, CNPq (Grant No. 432429/2016-6), and CAPES (Grant No. 88881.120309/2016-01) for financial support.

-
- [1] F. Varela, J. P. Lachaux, E. Rodriguez, and J. Martinerie, *Nat. Rev. Neurosci.* **2**, 229 (2001).
 - [2] G. Buzsaki, *Rhythms of the Brain* (Oxford University Press, New York, 2006).
 - [3] W. Singer, *Neuron Rev.* **24**, 49 (1999).
 - [4] P. Fries, *Trends Cogn. Sci.* **9**, 474 (2005).
 - [5] A. M. Bastos, J. Vezoli, and P. Fries, *Curr. Opin. Neurobiol.* **31**, 173 (2015).
 - [6] O. Jensen and A. Mazaheri, *Front. Human Neurosci.* **4**, 186 (2010).
 - [7] M. Bonnefond, S. Kastner, and O. Jensen, *eNeuro* **4**, 1 (2017).
 - [8] X. J. Wang, *Physiol. Rev.* **90**, 1195 (2010).
 - [9] G. Marsat and L. Maler, *J. Neurophysiol.* **104**, 2543 (2010).
 - [10] K. Padmanabhan and N. N. Urban, *Nat. Neurosci.* **13**, 1276 (2010).
 - [11] M. Savard, R. Krahe, and M. Chacron, *Neuroscience* **172**, 270 (2011).
 - [12] K. Angelo, E. A. Rancz, D. Pimentel, C. Hundahl, J. Hannibal, A. Fleischmann, B. Pichler, and T. W. Margrie, *Nature (London)* **488**, 375 (2012).
 - [13] S. J. Tripathy, K. Padmanabhan, R. C. Gerkin, and N. N. Urban, *Proc. Natl. Acad. Sci. USA* **110**, 8248 (2013).
 - [14] C. Beaulieu, *Brain Res.* **609**, 284 (1993).
 - [15] H. Markram, M. Toledo-Rodriguez, Y. Wang, A. Gupta, G. Silberberg, and C. Wu, *Nat. Rev. Neurosci.* **5**, 793 (2004).
 - [16] D. Golomb and J. Rinzel, *Phys. Rev. E* **48**, 4810 (1993).

- [17] M. Shamir and H. Sompolinsky, *Neural Comput.* **18**, 1951 (2006).
- [18] T. Pérez, C. R. Mirasso, R. Toral, and J. D. Gunton, *Philos. Trans. R. Soc. A* **368**, 5619 (2010).
- [19] J. F. Mejias and A. Longtin, *Phys. Rev. Lett.* **108**, 228102 (2012).
- [20] J. F. Mejias and A. Longtin, *Front. Comput. Neurosci.* **8**, 107 (2014).
- [21] K. L. Rossi, R. C. Budzinski, J. A. P. Silveira, B. R. R. Boaretto, T. L. Prado, S. R. Lopes, and U. Feudel, [arXiv:2003.03289](https://arxiv.org/abs/2003.03289).
- [22] F. Borges, P. Protachevich, R. Pena, E. Lameu, G. Higa, A. Kihara, F. Matias, C. Antonopoulos, R. de Pasquale, A. Roque *et al.*, *Physica A* **537**, 122671 (2020).
- [23] A. Renart, P. Song, and X.-J. Wang, *Neuron* **38**, 473 (2003).
- [24] J. Hass, S. Ardid, J. Sherfey, and N. Kopell, [bioRxiv 645663](https://doi.org/10.1101/465663) (2019).
- [25] H. U. Voss, *Phys. Rev. E* **61**, 5115 (2000).
- [26] F. S. Matias, L. L. Gollo, P. V. Carelli, S. L. Bressler, M. Copelli, and C. R. Mirasso, *NeuroImage* **99**, 411 (2014).
- [27] F. Montani, O. A. Rosso, F. S. Matias, S. L. Bressler, and C. R. Mirasso, *Phil. Trans. R. Soc. A* **373**, 20150110 (2015).
- [28] A. Brovelli, M. Ding, A. Ledberg, Y. Chen, R. Nakamura, and S. L. Bressler, *Proc. Natl. Acad. Sci. USA* **101**, 9849 (2004).
- [29] R. F. Salazar, N. M. Dotson, S. L. Bressler, and C. M. Gray, *Science* **338**, 1097 (2012).
- [30] H. U. Voss, *Phys. Rev. E* **64**, 039904(E) (2001).
- [31] H. U. Voss, *Phys. Rev. Lett.* **87**, 014102 (2001).
- [32] M. Cizak, O. Calvo, C. Masoller, C. R. Mirasso, and R. Toral, *Phys. Rev. Lett.* **90**, 204102 (2003).
- [33] C. Masoller and D. H. Zanette, *Physica A* **300**, 359 (2001).
- [34] E. Hernández-García, C. Masoller, and C. Mirasso, *Phys. Lett. A* **295**, 39 (2002).
- [35] J. Sausedo-Solorio and A. Pisarchik, *Phys. Lett. A* **378**, 2108 (2014).
- [36] S. Sivaprakasam, E. M. Shahverdiev, P. S. Spencer, and K. A. Shore, *Phys. Rev. Lett.* **87**, 154101 (2001).
- [37] M. Cizak, C. R. Mirasso, R. Toral, and O. Calvo, *Phys. Rev. E* **79**, 046203 (2009).
- [38] S. Tang and J. M. Liu, *Phys. Rev. Lett.* **90**, 194101 (2003).
- [39] M. Kostur, P. Hänggi, P. Talkner, and J. L. Mateos, *Phys. Rev. E* **72**, 036210 (2005).
- [40] T. Pyragienė and K. Pyragas, *Nonlinear Dyn.* **74**, 297 (2013).
- [41] A. Y. Simonov, S. Y. Gordleeva, A. Pisarchik, and V. Kazantsev, *JETP Lett.* **98**, 632 (2014).
- [42] Y. Hayashi, S. J. Nasuto, and H. Eberle, *Phys. Rev. E* **93**, 052229 (2016).
- [43] G. C. Dima, M. Copelli, and G. B. Mindlin, *Int. J. Bifurcation Chaos* **28**, 1830025 (2018).
- [44] M. A. Pinto, O. A. Rosso, and F. S. Matias, *Phys. Rev. E* **99**, 062411 (2019).
- [45] L. Dalla Porta, F. S. Matias, A. J. dos Santos, A. Alonso, P. V. Carelli, M. Copelli, and C. R. Mirasso, *Front. Syst. Neurosci.* **13**, 41 (2019).
- [46] F. S. Matias, P. V. Carelli, C. R. Mirasso, and M. Copelli, *Phys. Rev. E* **84**, 021922 (2011).
- [47] F. S. Matias, L. L. Gollo, P. V. Carelli, C. R. Mirasso, and M. Copelli, *Phys. Rev. E* **94**, 042411 (2016).
- [48] F. S. Matias, P. V. Carelli, C. R. Mirasso, and M. Copelli, *Phys. Rev. E* **95**, 052410 (2017).
- [49] C. R. Mirasso, P. V. Carelli, T. Pereira, F. S. Matias, and M. Copelli, *Chaos* **27**, 114305 (2017).
- [50] S. Petkoski, J. M. Palva, and V. K. Jirsa, *PLoS Comput. Biol.* **14**, e1006160 (2018).
- [51] J. N. Machado and F. S. Matias, *Phys. Rev. E* **102**, 032412 (2020).
- [52] N. Brunel, *J. Comput. Neurosci.* **8**, 183 (2000).
- [53] E. Izhikevich, *IEEE Trans. Neural Netw.* **14**, 1569 (2003).
- [54] N. Brunel and X.-J. Wang, *J. Neurophysiol.* **90**, 415 (2003).
- [55] I. D. Landau, R. Egger, V. J. Dercksen, M. Oberlaender, and H. Sompolinsky, *Neuron* **92**, 1106 (2016).
- [56] O. Yizhar, L. E. Fenno, M. Prigge, F. Schneider, T. J. Davidson, D. J. O'shea, V. S. Sohal, I. Goshen, J. Finkelstein, J. T. Paz *et al.*, *Nature (London)* **477**, 171 (2011).
- [57] F.-L. P. Carlos, M.-M. Ubrakitan, M. C. A. Rodrigues, M. Aguilar-Domingo, E. Herrera-Gutiérrez, J. Gómez-Amor, M. Copelli, P. V. Carelli, and F. S. Matias, *Phys. Rev. E* **102**, 032216 (2020).
- [58] G. A. Orban, K. Hoffmann, and J. Duysens, *J. Neurophysiol.* **54**, 1026 (1985).
- [59] L. Nowak, M. Munk, P. Girard, and J. Bullier, *Visual Neurosci.* **12**, 371 (1995).
- [60] D. Kerzel and K. R. Gegenfurtner, *Curr. Biol.* **13**, 1975 (2003).
- [61] D. Jancke, W. Erlhagen, G. Schöner, and H. R. Dinse, *J. Physiol.* **556**, 971 (2004).
- [62] G. D. Puccini, M. V. Sanchez-Vives, and A. Compte, *PLoS Comput. Biol.* **3**, e82 (2007).
- [63] L. M. Martinez, M. Molano-Mazo, X. Wang, F. T. Sommer, and J. Hirsch, *Neuron* **81**, 943 (2014).
- [64] J.-P. Rospars, A. Grémiaux, D. Jarriault, A. Chaffiol, C. Monsempe, N. Deisig, S. Anton, P. Lucas, and D. Martinez, *PLoS Comput. Biol.* **10**, e1003975 (2014).
- [65] N. Stepp and M. T. Turvey, *Cogn. Syst. Res.* **11**, 148 (2010).
- [66] N. Stepp and M. T. Turvey, *J. Exp. Psychol. Hum. Percept. Perform.* **43**, 914 (2017).
- [67] A. Kösem, A. Gramfort, and V. van Wassenhove, *Neuroimage* **92**, 274 (2014).
- [68] R. Vicente, L. L. Gollo, C. R. Mirasso, I. Fischer, and G. Pipa, *Proc. Natl. Acad. Sci. USA* **105**, 17157 (2008).
- [69] L. L. Gollo, C. Mirasso, O. Sporns, and M. Breakspear, *PLoS Comput. Biol.* **10**, e1003548 (2014).
- [70] E. Maris, T. Womelsdorf, R. Desimone, and P. Fries, *Neuroimage* **74**, 99 (2013).
- [71] E. Maris, P. Fries, and F. van Ede, *Trends Neurosci.* **39**, 86 (2016).
- [72] F. S. Matias, P. V. Carelli, C. R. Mirasso, and M. Copelli, *PloS ONE* **10**, e0140504 (2015).
- [73] A. Compte, M. V. Sanchez-Vives, D. A. McCormick, and X.-J. Wang, *J. Neurophysiol.* **89**, 2707 (2003).
- [74] A. Barbero-Castillo, P. Mateos-Aparicio, L. Dalla Porta, A. Camassa, L. Perez-Mendez, and M. V. Sanchez-Vives, Impact of GABA_A and GABA_B inhibition on cortical dynamics and perturbational complexity during synchronous and asynchronous activity (2020), doi:10.5281/zenodo.3856665.